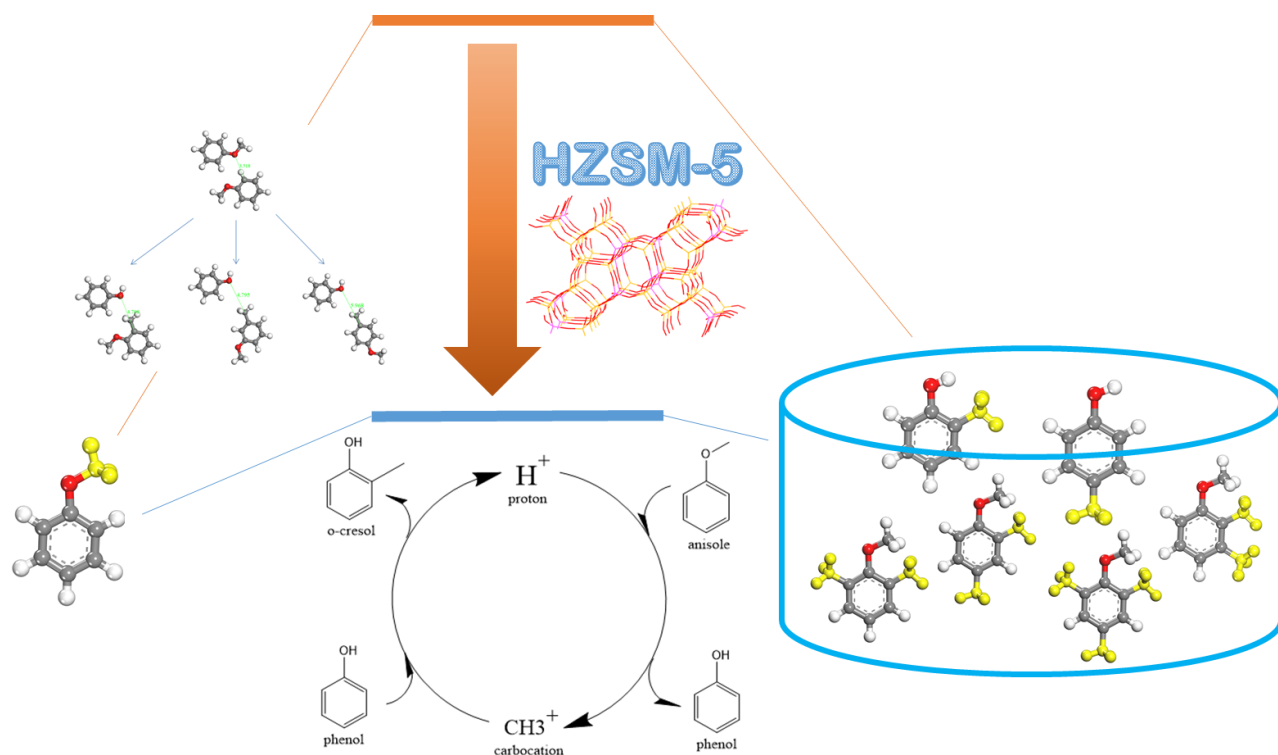


Table of Contents Entry

Acid catalyst promotes transmethylation in anisole decomposition through dual electrophilic attack mechanism, lowering intrinsic energy barriers by most 60 kcal/mol.



1 **Mechanism of transmethylation in anisole decomposition over Brønsted acid sites: Density**
2 **Functional Theory (DFT) study**

3 Jiajun Zhang^{ab}, Beatriz Fidalgo^b, Athanasios Kolios^b, Dekui Shen^{a*}, Sai Gu^c

4 * Corresponding author: Dekui Shen, Email: 101011398@seu.edu.cn

5 ^a Key Laboratory of Energy Thermal Conversion and Control of Ministry of Education,
6 Southeast University, Nanjing, China

7 ^b School of Water, Energy and Environment, Cranfield University, Cranfield, United Kingdom

8 ^c Faculty of Engineering and Physical Sciences, University of Surrey, Surrey, United Kingdom

9
10 **Abstract:** In this work, the mechanism and intrinsic reaction energy barriers of
11 transmethylation, as the initial stage of the catalytic and non-catalytic anisole decomposition,
12 were investigated by Density Functional Theory (DFT). Molecule analyses indicated that
13 methyl free radical transfer happened in the absence of catalyst, and the catalytic
14 transmethylation over Brønsted acid sites was considered based on the dual electrophilic
15 attack mechanism with protonation and carbocation substitution respectively. Reactions
16 modelling for the formation of methyl-contained compounds in both non-catalytic and catalytic
17 anisole decomposition indicated that the energy barriers were significantly decreased in the
18 presence of catalyst by 60 kcal/mol at the most in the case of o-cresol. The results also
19 revealed that the intrinsic transmethylation orientation preferred the ortho- and para-positions
20 on the acceptor compounds contained oxygen-rich substituents due to its large
21 electronegativity, and the lowest energy barrier was observed in the case of transmethylation
22 towards the para-position of the cresol molecule (54.1 kcal/mol).

23
24 **Key words:** lignin; catalytic decomposition; model compound; modelling; phenolic
25 compounds; substituent

26 **1. Introduction**

27 Lignin is an abundant aromatic-rich bio-resource; approximately 63 million tones are extracted
28 annually mainly from the pulp and paper industry ^{1,2}. The fast pyrolysis of lignin has been
29 investigated since the late 1970s, and is accepted as a feasible and viable route to convert

30 lignin into value added fuel additives³⁻⁵. However, the primary bio-oil produced from fast
31 pyrolysis cannot be directly used in fuel applications. This is because of its inadequate
32 properties, such as acidity, low calorific value, and low stability, which are a consequence of
33 its high oxygen content in composition. The effective removal of the oxygen by catalytic
34 upgrading is therefore crucial for making the bio-oil compatible with the existing fossil fuel
35 infrastructure and for widening its use^{6,7}. Catalytic cracking of bio-oil is one of the conversion
36 routes usually suggested for deoxygenation, and zeolites with dispersed Brønsted acid sites,
37 such as HZSM-5, have been proven as suitable catalysts for this process⁸⁻¹¹.

38 The methoxy group is an oxygen containing functional group which abundantly exists in
39 components present in the bio-oil obtained from the fast pyrolysis of lignin, such as anisole,
40 guaiacol, syringol and their derivatives¹². Understanding the reactivity of the methoxy group
41 is required to properly assess the complete catalytic upgrading process of these lignin-derived
42 aromatic compounds. Anisole is often used as a model compound to investigate the reactivity
43 of lignin-derived compounds containing the methoxy functional group, because this is the only
44 functional group present in the molecule¹³. Transmethylation reaction has been observed to
45 be the primary reaction taking place in anisole decomposition, leading to the prominent
46 production of phenolic compounds¹⁴⁻¹⁸.

47 Catalytic transmethylation over acid sites has been reported for phenol alkylation in the
48 presence of methanol¹⁹⁻²³. A few authors have described the transmethylation in the
49 decomposition of anisole over acid sites consisting of isomerization, dealkylation, and
50 intermolecular methyl transfer^{24,25}. However, available literature mainly focused on the
51 general study of pathways and kinetic parameters for the transmethylation reactions, with little
52 details on catalysis mechanisms despite their importance to understand the entire catalytic
53 process²⁶. Although it is widely accepted that Brønsted acid sites play a dominant role in
54 anisole decomposition^{14,19,24}, the precise mechanism for transmethylation over the acid sites
55 is still controversial. Different, and sometimes hardly consistent, reaction pathways and
56 mechanisms have been proposed for explaining the same chemical process in previous
57 studies¹⁹⁻²³. This might attributed to that transition state is key to understanding chemical
58 reaction mechanism, but it is extremely unstable and hard to capture by means of
59 experimental studies²⁷. Wang et al.¹⁶ have proposed hydrolysis as the first stage of the

60 anisole conversion, with little interaction of the acid sites, followed by the alkylation of phenol
61 with methanol. Thilakaratne et al.²⁸ proposed the transmethylation mechanism based on the
62 formation of a methenium ion during anisole decomposition on the Brønsted acid site. There
63 has been other study suggesting the formation of a methyl carbocation directly by the methyl
64 group in the anisole molecule^{14,24,25,28,29}, nevertheless, the studies have seldom addressed
65 how the carbocation is formed and to what extent it affects the transmethylation reaction. In
66 most previous studies, further evidence to prove the proposed mechanism regarding the
67 transmethylation, or to evaluate the reactions based on the mechanism were not provided.

68 Despite experimental results being highly valuable to understand the overall reaction and
69 products distribution at a macroscopic level, they present limitations in unravelling the
70 reaction mechanism at molecular level. Density Functional Theory (DFT) modelling is based
71 on the calculation of electrons interactions, and has been widely used as a systematic and
72 convincing approach in explaining molecular properties and mechanisms for many reactions
73³⁰⁻³⁴. Compared to experimental approach, DFT calculation can provide intrinsic information
74 of reactions regarding to detailed interaction between molecules and acid site, independently
75 of the very short life span of the transition states, radicals and ions existing in the reactions.

76 The microscale modelling of catalysis by DFT can also disregard complex impacts of
77 macroscale factors (e.g. framework effects) and allows focusing on the reaction regarding its
78 intrinsic properties. However, DFT calculation for transmethylation and related reactions has
79 little been reported in the literature.

80 The aim of this work is to investigate by means of DFT modelling the mechanism of
81 transmethylation as a primary reaction of the non-catalytic and catalytic decomposition of
82 anisole, and to identify the effects of Brønsted acid sites on transmethylation. Compounds
83 such as phenol, benzene, toluene, anisole, cresol, xylenol and tri-methyl phenol were
84 investigated. The transfer orientation preference of the electrophilic substituents on relevant
85 molecules was also studied. In addition, various possible reaction pathways of the
86 transmethylation reaction were evaluated to address energy barriers during formation of
87 major product compounds.

88 2. Computational method

89 The first-principles density functional theory plus dispersion (DFT-D) calculations were
90 implemented in the DMol³ module available in Materials Studio 2016 from BIOVIA^{35,36}. The
91 double numerical plus polarization (DNP) basis set was used to calculate the valence orbital
92 of all the atoms, including a polarization p-function on all hydrogen atoms. The numerical
93 basis sets in DMol³ minimize or even eliminate basis set superposition error (BSSE), in
94 contrast to Gaussian basis sets, in which BSSE can be a serious problem^{37,38}. Calculations
95 used the generalized gradient corrected approximation (GGA)³⁹ treated by the
96 Perdew–Burke–Ernzerhof (PBE) exchange-correlation potential with long-range dispersion
97 correction via Grimme’s scheme⁴⁰. The self-consistent field (SCF) procedure was used with a
98 convergence threshold of 10⁻⁶ au on the energy and electron density. Geometry optimizations
99 were performed with a convergence threshold of 0.002 Ha/Å on the gradient, 0.005 Å on
100 displacements, and 10⁻⁵ Ha on the energy. The real-space global cut-off radius was set to 5 Å.
101 In this study, no symmetry constraints were used for any cluster models. The transition state
102 was completely determined by the LST/QST method, and confirmed by the unique imaginary
103 frequency as shown in Table S1 in the supplementary information and Intrinsic reaction
104 coordinate (IRC) calculation. Milliken charges were assigned to each bond to address the
105 bond order, and Hirshfeld charges were assigned to each atom for the function selected as
106 the Fukui field⁴¹. Radical Fukui analysis was applied to the phenol molecule to establish its
107 reactivity to free radical attack in non-catalytic reactions. Electrophilic Fukui analysis was
108 applied to anisole and phenol molecules to determine their reactivity to carbocation attack in
109 catalytic reactions. The same computation condition was applied for both catalytic and non-
110 catalytic modellings; in the case of catalytic reactions modelling, mainly Brønsted acid was
111 considered. The initial configuration of the ZSM-5 catalysts was obtained from the siliceous
112 ZSM-5 crystal, and an 8T model was used to simulate the performance of a Brønsted acid
113 site^{31,32}. The energy barrier for transmethylation reaction was determined by the difference
114 between the transition state and reactant energies. The relative energy of the transition state
115 and product was defined as the energy difference with the reactant respectively. All the
116 energies were calculated at 0K to investigate the intrinsic reactions of transmethylation.

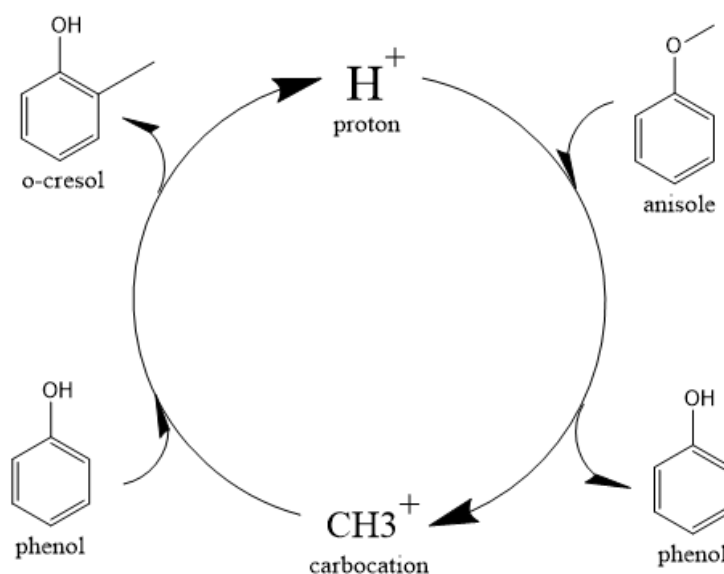
117 **3. Results and discussions**

118 **3.1 Mechanism for transmethylation in anisole decomposition**

119 The weakest bond in anisole molecule was observed for $C_{SP^3}-O$ (as shown in Fig S2(a), Bond
120 ID C8-O7), indicating that both the non-catalytic and catalytic thermal decomposition of
121 anisole is preferably initiated at this site ²⁹.

122 In the case of the non-catalytic decomposition of anisole, the molecule is subsequently
123 cracked into free radicals, with a methyl radical being formed, which substitutes the hydrogen
124 molecule on a phenol molecule to produce cresols ²⁹, and the free radical substitutions are
125 more likely to occur at the ortho-position and para-position of the phenol molecule (based on
126 radical Fukui analysis (Fukui (0)) to phenol molecule, shown in Fig S3(a)). A previous
127 experimental work by the group of J. Zhang et al ⁴² concluded the preferential formation of
128 cresols at temperatures lower than 650°C during the non-catalytic decomposition of anisole. It
129 should be noticed that due to there is no obvious intermediate compound existing in the non-
130 catalytic transmethylation reactions, they are more likely to occur as one step reactions.

131 In the case of the catalytic decomposition of anisole over Brønsted acid sites, it has been
132 largely recognized that the transmethylation reaction is induced by a proton that dissociates
133 from the acid site and launches an electrophilic attack on the reactant ^{14,43-46}. The
134 transmethylation mechanism is proposed to proceed through carbocation transfers in the
135 case of catalytic decomposition of anisole, as shown in Fig 1.



136

137 *Fig 1. Dual electrophilic attack mechanism of catalytic transmethylation*

138 The catalytic process of transmethylation can be divided into two steps. The first step consists
139 of the methyl group cleavage in the anisole molecule; an initial electrophilic attack is launched
140 by the proton dissociated from the catalyst acid site to the O atom (based on the electrophilic
141 Fukui (Fukui (-)) analysis to anisole molecule, as shown in Fig S2(b)), and the methyl
142 carbocation is released. A second electrophilic attack is launched by the methyl carbocation
143 group; the group is likely to substitute the hydrogen atom at the o- and p-positions on the
144 phenol ring (based on the electrophilic Fukui analysis (Fukui (-)) to phenol molecule, as
145 shown in Fig S3(b)). The displaced free proton simultaneously interacts with the catalyst to
146 recover the Brønsted acid site and maintain the catalytic activity throughout the reaction.
147 Transition state compounds normally exist for a very short time due to instability; however, the
148 methyl carbocation attached to the active site during the transmethylation process is a
149 relatively stable structure with zero valent. Consequently, it can be considered as an
150 intermediate compound, rather than a transition state compound, therefore it is possible to
151 consider the methyl carbocation cleavage and the carbocation substitution reactions as
152 separate steps in the catalytic transmethylation. The mechanism described in Fig 1 shows
153 that the use of Brønsted acid catalyst replaces the one-step reaction of direct methyl free
154 radical transfer observed for the non-catalytic reaction by a two-step process [25]. The
155 mechanism also shows constant maintenance of acid sites in the catalyst by proton recovery
156 throughout the reaction. Further reaction modelling was carried out considering the
157 mechanism proposed here.

158 It is worth noting that in both non-catalytic and catalytic decomposition of anisole, the methyl
159 group transfers not only to phenol but also to other compounds such as benzene, toluene,
160 and even non-decomposed anisole present in the reaction media ⁴². All the transmethylation
161 processes are initiated from methyl cleavage.

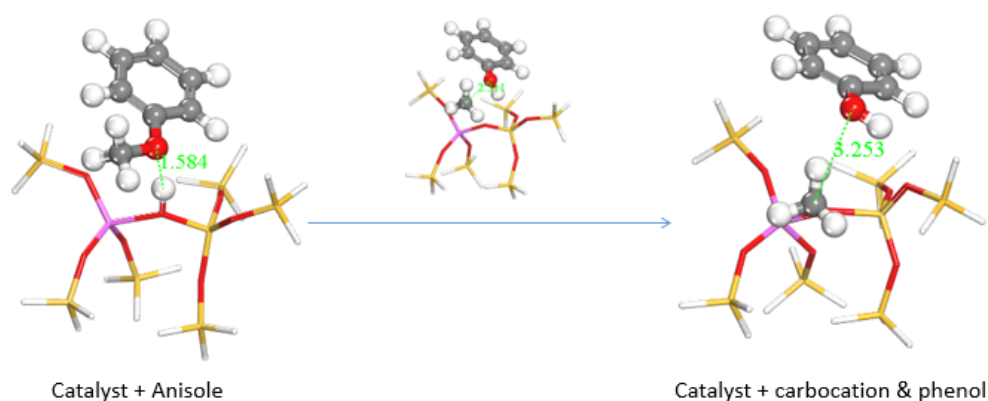
162 **3.2 Modelling of non-catalytic and catalytic transmethylation of anisole to phenol**

163 The transmethylation reactions with a phenol molecule in the non-catalytic and catalytic
164 decomposition of anisole were modelled. Both non-catalytic and catalytic transmethylation
165 models were built by locating equidistantly the reactant molecules (about 3Å) to minimize any
166 possible position-related errors. The catalytic transmethylation was modelled based on the

167 dual electrophilic attack mechanism proposed in Fig 1, considering the system containing
168 methyl carbocation on the acid site as the intermediate compound (see Fig 2). The modelling
169 was implemented in two stages: methyl carbocation cleavage from anisole over the catalyst
170 active site, and transfer of the carbocation to the surrounding molecules. The transition states
171 for both stages are denoted as TS1 and TS2 respectively. The non-catalytic transmethylation
172 model was built according to the free radical mechanism, and the transition state of the
173 reaction is denoted as TS. The cleavage energy of the carbocation from the anisole molecule
174 (for TS1) and the energy barriers for the methyl carbocation transfer to ortho-, meta-, and
175 para-positions of phenol (for TS2) during the catalytic transmethylation of anisole to form
176 cresol via phenol, as predicted by the model, are shown in Fig 3. The transition state (TS) and
177 corresponding energy barriers for the non-catalytic transmethylation of anisole to form n-
178 cresol are shown for comparison.

179 As can be seen in Fig 3, the transmethylation to the ortho-position of phenol presented a
180 lower energy barrier than the meta-position and para-position transfers both in non-catalytic
181 and catalytic decomposition. This result indicates that ortho-position transmethylation is more
182 likely to occur to the phenol molecule, which agrees with the experimental observations found
183 elsewhere ⁴². In short, experiments showed that o-cresol was formed at a lower temperature
184 (550°C) than p-cresol (600°C) in non-catalytic anisole decomposition, and most multi-methyl
185 phenolic compounds presented the ortho-position occupied by a methyl group in the catalytic
186 anisole decomposition ⁴². In addition, the model pointed to the highest energy barrier for the
187 meta-position transfer. This is in agreement with experimental results, which exhibited no
188 evidence of m-cresol formation ⁴². However, it should be noted that the results in this study
189 show the intrinsic properties of the reaction, and the experimental yields obtained are
190 normally subjected to other effects, such as the framework topology effects of different
191 zeolites. For example, shape selectivity of microporous zeolites plays a key role in the
192 catalyst promoting the production of para-cresol ²⁵.

Transition state compound of catalytic methyl cleavage (TS1)

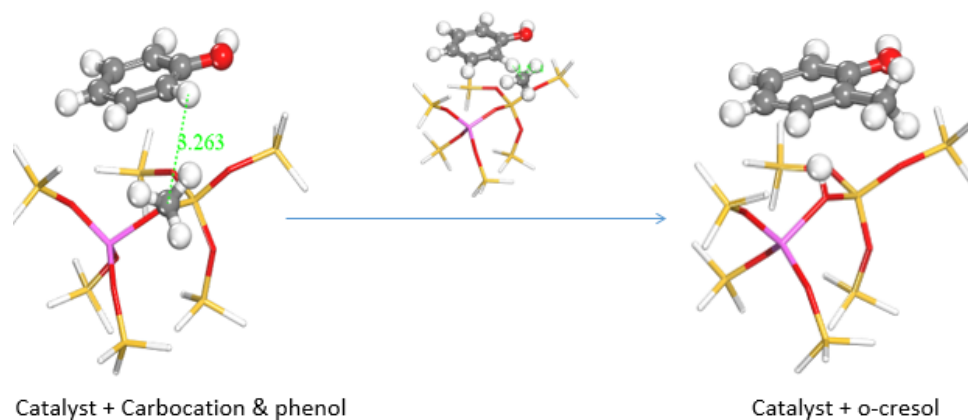


193

194

(a)

Transition state compound of carbocation transfer (TS2)



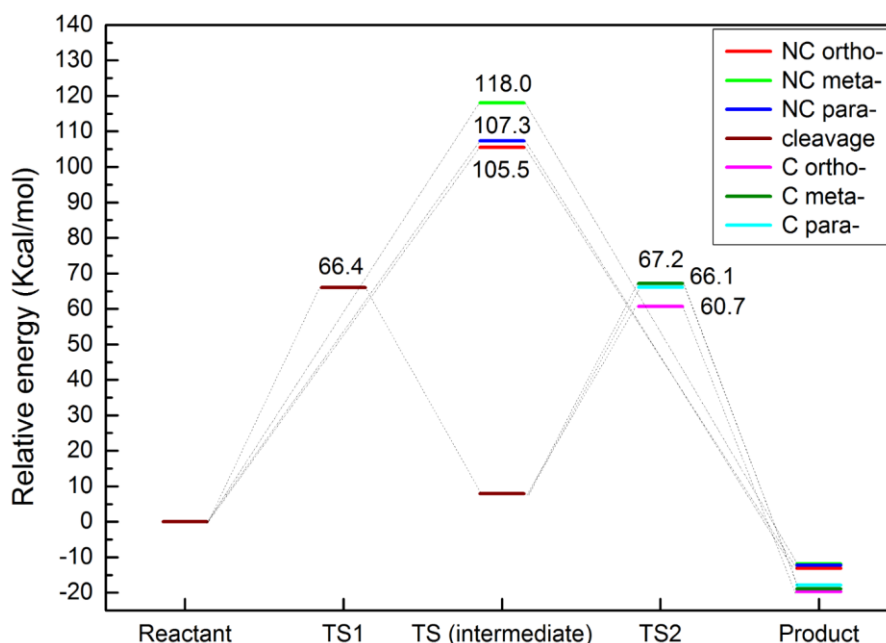
195

196

(b)

197 *Fig 2. (a) CSP3-O bond (C8-O7) cleavage and carbocation formation; (b) Methyl carbocation*
198 *transfer to ortho-position of phenol (transfers to meta- and para-positions are not shown here).*
199 *Atoms are colored as follows: carbon atom (grey), hydrogen atom (light grey), oxygen atom*
200 *(red), silica atom (yellow) and aluminum atom (pink).*

201 The model also predicted that the energy barrier for the methyl cleavage in the presence of
202 the catalyst was 66.4 kcal/mol, which is much lower than the energy barrier values of the non-
203 catalytic process. Moreover, compared to the non-catalytic process, the energy barrier for
204 catalytic transmethylation to ortho-position decreased from 105.5 kcal/mol to 60.7 kcal/mol,
205 and those for para- and meta-positions dropped from 107.3 kcal/mol to 66.1 kcal/mol and
206 from 118.0 kcal/mol to 67.2 kcal/mol respectively. These results are also in line with
207 experimental data which showed that a lower temperature (approximately by 150°C) was
208 required to achieve a similar conversion ratio during the catalytic decomposition of anisole
209 compared to non-catalytic decomposition ⁴².



210

211 *Fig 3. Energy barriers for transmethylation reactions of anisole to cresol (via phenol). (C*
 212 *denotes to catalytic transmethylation; NC denotes to non-catalytic transmethylation)*

213 **3.3 Modelling of non-catalytic and catalytic transmethylation of anisole to other**
 214 **acceptor molecules**

215 Besides the cresol, the transmethylation process also gives rise to other methyl substituted
 216 compounds⁴². Therefore, transmethylation reactions with other acceptor molecules were
 217 modelled to assess the reactivity of these intermediate compounds, and the selectivity of the
 218 resulting products. The formation of toluene, methyl anisole, xylene, xylenol, and trimethyl-
 219 phenol due to the addition of a methyl group to benzene, anisole, toluene, cresol and xylenol
 220 respectively were also modelled. The energy barriers for the different reactions pathways in
 221 non-catalytic and catalytic decomposition of anisole are shown in Table 1.

222 In the case of non-catalytic decomposition, the energy barriers of transmethylation changed
 223 significantly, depending on the acceptor molecules. This is related to the fact that the
 224 substituents on the molecule affect the electron distribution in the aromatic ring, giving rise to
 225 the site migration of substituted reactions⁴⁷. Anisole, toluene and phenolic compounds
 226 showed energy barrier values between 105.7 and 121.1 kcal/mol in the non-catalytic
 227 transmethylation (Table 1), and the energy barrier for the methyl transfer to benzene in the
 228 non-catalytic reaction was the highest for 126.4 kcal/mol.

229 It is found the molecules containing branch chain substituents, especially oxygen-rich chains
 230 such as hydroxy and methoxy functional groups, are more readily to accept methyl radicals.

231 The branch chains may have impact on the π -bond of the benzene ring, making the ring more
 232 susceptible to methyl attack especially at the ortho- and para-positions, while the benzene
 233 ring without branch chains may have smaller electron density, so that is more stable to radical
 234 attack ⁴⁸.

235 It was observed that transmethylation to phenol and o-cresol exhibited intrinsic preference in
 236 the ortho- and para-positions, which is in line with the results from the Fukui analyses for
 237 electrophilic attack to phenol molecule (Fig S3(b)). On the other hand, toluene and anisole
 238 showed moderate difference (within 4.1 kcal/mol) in position preference for non-catalytic
 239 transmethylation. This is because the free pair of electrons in the oxygen of the hydroxyl
 240 group are more likely to move to the ring, and consequently affect the ring property; while less
 241 electron migration and less impact onto the ring occurs with the methyl group attached either
 242 directly to the ring (in the case of toluene) or to the oxygen (in the case of anisole) ⁴⁹.

243 *Table 1. Energy barrier for the different reaction pathways of transmethylation in non-catalytic*
 244 *and catalytic decomposition of anisole*

Reactant	Via	Product	Orientation	Energy Barrier (kcal/mol)		
				Non-catalytic (TS)	Catalytic	
					Cleavage (TS1)	Methyl cation transfer (TS2)
Anisole	Phenol	Cresol	Ortho	105.5	60.7	
			Meta	118.0	67.2	
			Para	107.3	66.1	
			Ortho	107.2	60.4	
	o-Cresol	Xylenol	Meta	121.1	61.8	
			Para	107.0	54.1	
	2,4-Xylenol	2,4,6-Phenol	Ortho	114.3	66.4	
			Meta	110.0	59.9	
	Benzene	Toluene	-	126.4	73.5	
	Toluene	Xylene	Ortho	108.1	71.2	
Meta			112.2	68.3		

		Para	109.5	70.8
		Ortho	106.9	63.3
Anisole	Methyl- anisole	Meta	105.7	67.0
		Para	108.3	71.7

245 In the case of catalytic reactions, the presence of the acid catalyst decreased notably the
246 energy barrier values, exhibiting a big influence on promoting transmethylation. The
247 decreases in the energy barrier was observed range from 36.6 kcal/mol (transmethylation to
248 para position of anisole) to 59.3 kcal/mol (transmethylation to meta position of o-cresol). The
249 transmethylation to benzene is found had the highest energy barrier for 73.5 kcal/mol, even
250 though it has been diminished by roughly 53 kcal/mol compared to the non-catalytic process,
251 this indicates the stability of the benzene ring to electrophilic attack compared to other branch
252 chain contained compounds. In the case of the transmethylation to toluene, the model also
253 predicted a decrease in the energy barrier value for each of the position transfers when using
254 a catalyst (ranging between 68.3kcal/mol and 71.2kcal/mol), but the predicted energy barriers
255 are higher than those for most oxygen contained compounds, regardless of the position
256 transfer. It is also noted that transmethylation to anisole at the ortho-position to produce
257 methyl-anisole exhibited a similar energy barrier value to other phenolic intermediate
258 compounds (63.3 kcal/mol). This result suggests that the presence of sole methyl group
259 attached to the aromatic ring has limited effect on the molecules to accept electrophilic
260 substitution by methyl carbocation, this may attribute to the lower electronegativity of the
261 methyl group than that of the oxygen contained functional groups⁵⁰. In other words, hydroxyl
262 and methoxyl groups are the most likely ones to promote the reactivity of the aromatic ring,
263 followed by methyl group. Benzene molecule itself is the least reactive compound among the
264 evaluated molecules in the catalytic transmethylation over the Brønsted acid sites. At a
265 macroscopic level, it can be inferred that in the catalytic decomposition of anisole, majority of
266 toluene and xylene are probably produced from the deoxygenation of cresols and xylenols,
267 rather than from the transmethylation to benzene over the Brønsted acid sites.

268 Compared to AHs, methyl phenolic compounds, i.e. phenol, cresol and xylenol, are found to
269 be prone to accept electrophilic substitution at all positions, even though a slight preference
270 (values difference lower than 8 kcal/mol) for ortho- and para-positions were observed in the

271 case of phenol and cresol. Among all the evaluated compounds, these molecules accept
272 methyl carbocation at the lowest energy barrier values. Transmethylation for cresol into
273 xylenol presented energy barriers ranging from 54.1 kcal/mol (p-position transfer) to 61.8
274 kcal/mol (m-position transfer). Transmethylation to convert xylenol into 2,3,6-methyl phenol
275 and 2,4,6-methyl phenol exhibited similar energy barriers at around 60 kcal/mol. These
276 results well illustrate the experimental results during catalytic decomposition of anisole in
277 which the abundant production of multi-methyl phenolic compounds and the typical position
278 preference was observed ⁴². The formation of these multi-methyl phenolic compounds from
279 anisole depends on the initial formation of cresol.

280 **4 CONCLUSION**

281 This work presents the DFT modelling of the transmethylation as the primary reaction taking
282 place in both non-catalytic and catalytic anisole decomposition. Methyl radical cleavage led to
283 the transmethylation process in non-catalytic transmethylation, which primarily took place with
284 the methyl free radical transfer. In catalytic transmethylation, reactants interacted with the
285 Brønsted acid sites present in the catalyst. The catalytic transmethylation was initiated by the
286 Brønsted acid proton electrophilic attack at the oxygen atom of anisole, followed by a
287 carbocation substitution. A dual electrophilic attack mechanism was proposed for the catalytic
288 transmethylation. Transmethylation reactions modelling, based on the proposed mechanism,
289 proved that the Brønsted acid catalyst could significantly lower the reaction energy barrier for
290 all reactant compounds investigated due to changes in the reaction pathways. Most of the
291 energy barriers for the evaluated transmethylation reactions decreased more than 40 kcal/mol
292 when considering the catalytic effect, the highest decrease being observed in the case of o-
293 cresol (around 60 kcal/mol). Furthermore, both non-catalytic and catalytic transmethylation
294 exhibited target molecule preference, depending on the original substituents of the acceptor,
295 and transmethylation to most compounds showed preference for the ortho- and para-
296 positions. Non-catalytic transmethylation to compounds with oxygen-rich substituents
297 generally showed lower energy barriers. In the catalytic decomposition of anisole, the
298 presence of oxygen-rich substituents also enhanced the reactivity of the ring, especially for
299 phenolic compounds at the ortho- and para-positions. The lowest energy barrier was

300 observed in the case of transmethylation towards the para-position of the cresol molecule
301 (54.1 kcal/mol).

302 **AUTHOR INFORMATION**

303 **Corresponding Author**

304 D.S.: 101011398@seu.edu.cn

305 **Author Contributions**

306 All authors have given approval to the final version of the manuscript.

307 **Notes**

308 The authors declare no competing financial interest.

309 **ACKNOWLEDGEMENT**

310 The authors would like to acknowledge financial support from the National Natural Science
311 Foundation of China (project references: 51476034 and 51628601), Natural Science
312 Foundation of Jiangsu Province (project reference: BK20161423), and the FP7 Marie Curie
313 iComFluid (project reference: 312261).

314 **REFERENCES**

- 315 1 W. Boerjan, J. Ralph and M. Baucher, *Annu. Rev. Plant Biol.*, 2003, **54**, 519–546.
- 316 2 C. S. Lancefield and N. J. Westwood, *Green Chem.*, 2015, **17**, 4980–4990.
- 317 3 A. V. Bridgwater, *Biomass and Bioenergy*, 2012, **38**, 68–94.
- 318 4 A. V. Bridgwater and G. V. C. Peacocke, *Renew. Sustain. energy Rev.*, 2000, **4**, 1–73.
- 319 5 K. A. Jung, S. H. Woo, S.-R. Lim and J. M. Park, *Chem. Eng. J.*, 2015, **259**, 107–116.
- 320 6 L. Zhang, R. Liu, R. Yin and Y. Mei, *Renew. Sustain. Energy Rev.*, 2013, **24**, 66–72.
- 321 7 C. Liu, H. Wang, A. M. Karim, J. Sun, Y. Wang, M. Karim Ayman, J. Sun and Y. Wang,
322 *Chem. Soc. Rev.*, 2014, **43**, 7594–7623.
- 323 8 S. Vichaphund, D. Aht-ong, V. Sricharoenchaikul and D. Atong, *Renew. Energy*, 2014,
324 **65**, 70–77.
- 325 9 C. Mukarakate, J. D. McBrayer, T. J. Evans, S. Budhi, D. J. Robichaud, K. lisa, J. ten

- 326 Dam, M. J. Watson, R. M. Baldwin and M. R. Nimlos, *Green Chem.*, 2015, **17**, 4217–
327 4227.
- 328 10 C. Mukarakate, X. Zhang, A. R. Stanton, D. J. Robichaud, P. N. Ciesielski, K. Malhotra,
329 B. S. Donohoe, E. Gjersing, R. J. Evans, D. S. Heroux, R. Richards, K. Lisa and M. R.
330 Nimlos, *Green Chem.*, 2014, **16**, 1444.
- 331 11 G. Yildiz, M. Pronk, M. Djokic, K. M. Van Geem, F. Ronsse, R. Van Duren and W.
332 Prins, *J. Anal. Appl. Pyrolysis*, 2013, **103**, 343–351.
- 333 12 D. K. Shen, S. Gu, K. H. Luo, S. R. Wang and M. X. Fang, *Bioresour. Technol.*, 2010,
334 **101**, 6136–6146.
- 335 13 S. J. Hurff and M. T. Klein, *Ind. Eng. Chem. Fundam.*, 1983, **22**, 426–430.
- 336 14 Q. Meng, H. Fan, H. Liu, H. Zhou, Z. He, Z. Jiang, T. Wu and B. Han, *ChemCatChem*,
337 2015, **7**, 2831–2835.
- 338 15 T. Prasomsri, A. T. To, S. Crossley, W. E. Alvarez and D. E. Resasco, *Appl. Catal. B*
339 *Environ.*, 2011, **106**, 204–211.
- 340 16 K. Wang, X. Dong, Z. Chen, Y. He, Y. Xu and Z. Liu, *Microporous Mesoporous Mater.*,
341 2014, **185**, 61–65.
- 342 17 J. Cornella, E. Gómez-Bengoa and R. Martin, *J. Am. Chem. Soc.*, 2013, **135**, 1997–
343 2009.
- 344 18 C. Mackie, R. Doolan and F. Nelson, *J. Phys. Chem. C*, 1989, **93**, 664–670.
- 345 19 M. E. Sad, C. L. Padró and C. R. Apesteguía, *Catal. Today*, 2008, **133–135**, 720–728.
- 346 20 J. Xu, A. Z. Yan and Q. H. Xu, *Appl. Catal.*, 1999, **10**, 983–986.
- 347 21 W. Wang, P. L. De Cola, R. Glaeser, I. I. Ivanova, J. Weitkamp and M. Hunger, *Catal.*
348 *Commun.*, 2004, **94**, 119–123.
- 349 22 M. Bregolato, V. Bolis, C. Busco, P. Ugliengo, S. Bordiga, F. Cavani, N. Ballarini, L.
350 Maselli, S. Passeri and I. Rossetti, *J. Catal.*, 2007, **245**, 285–300.
- 351 23 K. G. Bhattacharyya, A. K. Talukdar, P. Das and S. Sivasanker, *J. Mol. Catal. A*
352 *Chem.*, 2003, **197**, 255–262.

353 24 M. E. Sad, C. L. Padró and C. R. Apesteguía, *J. Mol. Catal. A Chem.*, 2010, **327**, 63–
354 72.

355 25 X. Zhu, R. G. Mallinson and D. E. Resasco, *Appl. Catal. A Gen.*, 2010, **379**, 172–181.

356 26 N. Ballarini, F. Cavani, L. Maselli, A. Montaletti, S. Passeri, D. Scagliarini, C. Flego
357 and C. Perego, *J. Catal.*, 2007, **251**, 423–436.

358 27 J. H. Baraban, P. B. Changala, G. C. Mellau, J. F. Stanton, A. J. Merer and R. W.
359 Field, *Science (80-.)*, 2015, **350**, 1338–1342.

360 28 R. Thilakaratne, J.-P. Tessonier and R. C. Brown, *Green Chem.*, 2016, **18**, 2231–
361 2239.

362 29 G. Li, L. Li, L. Shi, L. Jin, Z. Tang, H. Fan and H. Hu, *Energy & Fuels*, 2014, **28**, 980–
363 986.

364 30 Z. Geng, M. Zhang and Y. Yu, *Fuel*, 2012, **93**, 92–98.

365 31 Y. Huang, X. Dong, M. Li, Y. Yu, J. Gao, Y. Zheng, G. B. Fitzgerald, J. de Joannis, Y.
366 Tang, I. E. Wachs, S. G. Podkolzin, Y. Huang, X. Dong, M. Li, M. Zhang and Y. Yu,
367 *Catal. Sci. Technol.*, 2015, **5**, 1093–1105.

368 32 Y. Huang, X. Dong, M. Li, M. Zhang and Y. Yu, *RSC Adv.*, 2014, **4**, 14573.

369 33 J. Gao, Y. Zheng, G. B. Fitzgerald, J. de Joannis, Y. Tang, I. E. Wachs and S. G.
370 Podkolzin, *J. Phys. Chem. C*, 2014, **118**, 4670–4679.

371 34 Z. K. Li, Z. M. Zong, H. L. Yan, Y. G. Wang, X. Y. Wei, D.-L. Shi, Y. P. Zhao, C. L.
372 Zhao, Z. S. Yang and X. Fan, *Fuel*, 2014, **120**, 158–162.

373 35 B. Delley, *J. Chem. Phys.*, 1990, **92**, 508–517.

374 36 B. Delley, *J. Chem. Phys.*, 2000, **113**, 7756.

375 37 M. Elanany, M. Koyama, M. Kubo, P. Selvam and A. Miyamoto, *Microporous*
376 *mesoporous Mater.*, 2004, **71**, 51–56.

377 38 B. Kalita and R. C. Deka, *Eur. Phys. J. D*, 2009, **53**, 51–58.

378 39 J. P. Perdew, K. Burke and M. Ernzerhof, *Phys. Rev. Lett.*, 1996, **77**, 3865–3868.

379 40 S. Grimme, *J. Comput. Chem.*, 2006, **27**, 1787–1799.

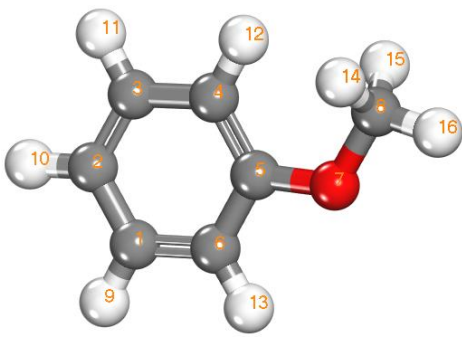
- 380 41 F. L. Hirshfeld, *Theor. Chim. Acta*, 1977, **44**, 129–138.
- 381 42 J. Zhang, B. Fidalgo, D. Shen, R. Xiao and S. Gu, *J. Anal. Appl. Pyrolysis*, 2016, **122**,
382 323–331.
- 383 43 J. F. Haw, B. R. Richardson, I. S. Oshiro, N. D. Lazo and J. a. Speed, *J. Am. Chem.*
384 *Soc.*, 1989, **111**, 2052–2058.
- 385 44 B. R. Richardson, N. D. Lazo, P. D. Schettler, J. L. White and J. F. Haw, *J. Am. Chem.*
386 *Soc.*, 1990, **112**, 2886–2891.
- 387 45 E. J. Munson, T. Xu and J. F. Haw, *J. Chem. Soc. Chem. Commun.*, 1993, 75–76.
- 388 46 E. J. M. and J. F. H. Teng Xu, Jinhua Zhang, *Chem. Commun.*, 1994, 2733–2735.
- 389 47 F. L. Lambert, *J. Chem. Educ.*, 1958, **35**, 342–343.
- 390 48 T. Phuong, *J. Catal.*, 1986, **102**, 456–459.
- 391 49 X. Zhu, L. L. Lobban, R. G. Mallinson and D. E. Resasco, *J. Catal.*, 2011, **281**, 21–29.
- 392 50 F. De Proft, W. Langenaeker and P. Geerlings, *J. Phys. Chem.*, 1993, **97**, 1826–1831.

Supplementary Information

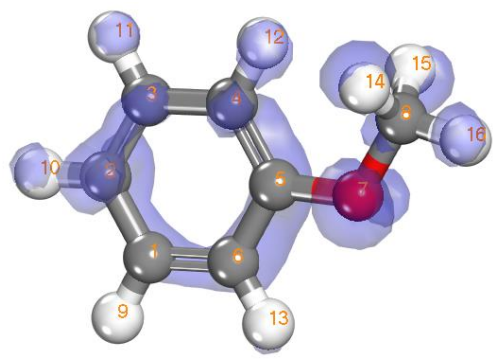
Table S1: Unique imaginary frequency identified for each transition state of the reactions for both non-catalytic and catalytic transmethylation

Reactant	Via	Product	Orientation	Imaginary frequency (Frequency(1/cm); Intensity(km/mol))		
				Non-catalytic (TS)	Catalytic	
					Cleavage (TS1)	Methyl cation transfer (TS2)
anisole	phenol	Cresol	Ortho	-15.49/0.03		-352.36/6.86
			Meta	-11.96/0.14		-285.63/7.12
			Para	-10.15/0.11		-435.58/5.90
	o-cresol	Xylenol	Ortho	-304.25/658.68		-345.63/7.72
			Meta	-144.6/1.40		-311.78/158.17
			Para	-270.32/163.89		-343.56/192.81
	2,4-xylenol	2,4,6-phenol	Ortho	-237.38/453.09		-171.58/6.64
	2,6-xylenol	2,3,6-phenol	Meta	-229.42/129.61	-331.54/99.74	-511.45/499.08
	benzene	Toluene	-	-686.39/37.85		-233.06/16.67
	toluene	Xylene	Ortho	-244.71/129.42		-138.44/101.67
			Meta	-240.01/87.44		-320.08/188.36
			Para	-36.49/27.64		-302.45/185.02
anisole	methyl-anisole	Ortho	-283.22/185.03		-98.98/4.73	
		Meta	-6823.26/7.10		-313.60/67.33	
		Para	-267.68/159.39		-309.34/2.79	

Fig S2. (a) Mulliken bond order of the anisole molecule for the transmethylation reaction; (b) Fukui indices of anisole atoms under electrophilic attack (Fukui (-)). Isovalue 0.035. Atoms are colored as follows: carbon atom (grey), hydrogen atom (white) and oxygen atom (red)

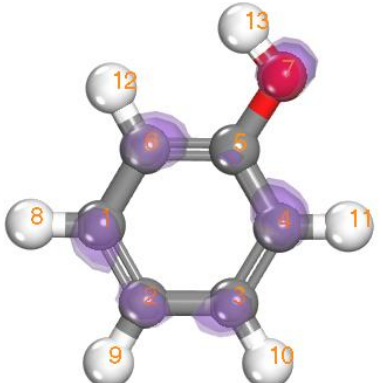
	Bond ID	Mulliken Bond order
	C8-O7	0.515
	C5-O7	0.668
	C8-H14	0.798
	C8-H15	0.799
	C6-H13	0.813
	C4-H12	0.814
	C3-H11	0.821
	C1-H9	0.824
	C2-H10	0.825
	C8-H16	0.826
	C4-C5	1.003
	C3-C4	1.025
	C5-C6	1.030
	C1-C2	1.032
	C1-C6	1.054
C2-C3	1.063	

(a)

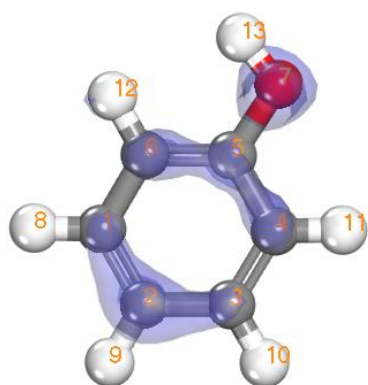
	Atom	Fukui (-) index
	O7	0.129
	C2	0.125
	C6	0.086
	C5	0.075
	C4	0.072
	C3	0.071
	C1	0.061
	H10	0.057
	H11	0.046
	H13	0.046
	H9	0.044
	H12	0.040
	H15	0.038
	H14	0.037
	H16	0.036
	C8	0.035

(b)

Fig S3. Fukui indices for (a) radical attack on phenol molecule (Fukui (0)), and (b) electrophilic attack on phenol molecule (Fukui (-)). Isovalue 0.035. Atoms are colored as follows: carbon atom (grey), and hydrogen atom (white) and oxygen atom (red)

	Atom	Fukui (0) index
	C4	0.105
	O7	0.103
	C2	0.102
	C6	0.100
	C1	0.099
	C3	0.095
	C5	0.073
	H8	0.057
	H10	0.056
	H11	0.056
	H9	0.055
	H12	0.055
	H13	0.044

(a)



Atom	Fukui (-) index
O7	0.152
C2	0.136
C4	0.089
C5	0.089
C6	0.083
C1	0.073
C3	0.068
H9	0.061
H13	0.055
H11	0.050
H8	0.049
H10	0.048
H12	0.048

(b)

2017-08-15

Mechanism of transmethylation in anisole decomposition over Brønsted acid sites: Density Functional Theory (DFT) study

Zhang, Jiajun

Royal Society of Chemistry

Zhang J, Fidalgo B, Kolios A, Shen D, Gu S, Mechanism of transmethylation in anisole decomposition over Brønsted acid sites: Density Functional Theory (DFT) study, Sustainable Energy & Fuels, Vol. 1, Issue 8, 2017, pp. 1788-1794

<http://dx.doi.org/10.1039/C7SE00280G>

Downloaded from CERES Research Repository, Cranfield University